

Engineering Curvature Induced Anisotropy in Thin Ferromagnetic Films

Oleg A. Tretiakov*

*Institute for Materials Research, Tohoku University, Sendai 980-8577, Japan and
School of Natural Sciences, Far Eastern Federal University, Vladivostok 690950, Russia*

Massimiliano Morini

Universita di Parma, Parma, Italy

Sergiy Vasylykevych and Valeriy Slastikov

School of Mathematics, University of Bristol, Bristol, BS8 1TW, UK

(Dated: October 18, 2016)

The large curvature effects on micromagnetic energy of a thin ferromagnetic film with nonlocal dipolar energy are considered. We predict that the dipolar interaction and surface curvature can produce perpendicular anisotropy which can be controlled by engineering a special type of periodic surface shape structure. Similar effects can be achieved by a significant surface roughness in the film. We show that in general the anisotropy can point in an arbitrary direction depending on the surface curvature. We provide simple examples of these periodic surface structures to demonstrate how to engineer particular anisotropies in the film.

The puzzle of perpendicular magnetic anisotropy (PMA) origin in thin ferromagnetic films has a long history, dating back to Néel who was the first to address it [1]. Later, there have been several other attempts in this direction [2–6]. In particular, in multilayers consisting of alternating ferromagnetic and heavy-metal (such as Pt) layers, PMA was attributed to strong spin-orbit interaction at the interfaces [7–12]. However, in thin magnetic films PMA may exist without additional heavy-metal layer [13], which enhances spin-orbit interaction in the system, thus pointing to a more general perpendicular anisotropy mechanism.

Recent studies of magnetic structures with large-scale smoothly varying curvature have shown that the magnetization prefers to stay in tangential plane of the surface [14–17]. However, nowadays the thickness of magnetic films often reaches just a few monolayers, in which case the surface roughness may lead to large and rapid modulations of geometric curvature. This can significantly modify the magnetic properties and, in fact, be responsible for the PMA in thin ferromagnetic films.

In this Letter we aim to understand the effect of surface roughness on the shape anisotropy and demonstrate the formation mechanism of perpendicular or any other given direction of magnetic anisotropy by means of surface engineering of a thin magnetic film. The proposed mechanism does not require any spin-orbit coupling and is related solely to the interplay of surface curvature and dipolar interactions in the film. This possibility may open up a direction to tailor the interfacial magnetic anisotropy in thin ferromagnetic films without any additional layers of heavy metal, which, in turn, may lead to simpler and cheaper ways to engineer systems with any given anisotropy.

Recently the curvature effects in thin magnetic films have become more accessible due to experimental ad-

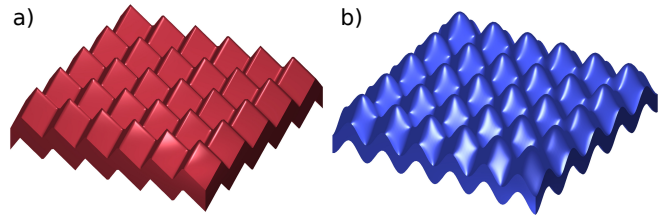


FIG. 1. Examples of engineered periodic magnetic films. (a) The film consisting of pyramids. (b) The film consisting of $\sin^2 x_1 \sin^2 x_2$ shapes.

vances in flexible electronics [18–22], making the proposed method to control the anisotropy experimentally viable in the near future. Moreover, our findings imply that similar effects might be observed in thin films with significant surface roughness.

We obtain our results by employing asymptotic homogenization to tackle the physics of magnetic surfaces with small rapid periodic modulation. Physically the problem is associated with two scales, the larger scale is given by the size of the film’s domain where we aim to determine the anisotropy, whereas the smaller one is given by the size of film’s curvature modulation. The latter scale should be generally much smaller to have a nontrivial effect on anisotropy, which can be homogenized over the larger film’s scale. Formally, the method of asymptotic homogenization proceeds by introducing the fast variable $\mathbf{y} = \mathbf{x}/\varepsilon$ and performing an expansion of unit magnetization \mathbf{M} in small parameter ε :

$$\mathbf{M}_\varepsilon(\mathbf{x}) = \mathbf{M}_0(\mathbf{x}) + \varepsilon \mathbf{M}_1(\mathbf{x}, \mathbf{y}) + O(\varepsilon^2), \quad (1)$$

which generates a hierarchy of problems. The homogenized equation is obtained and the effective coefficients are determined by solving the so-called “cell problems” for the function $\mathbf{M}_1(\mathbf{x}, \mathbf{x}/\varepsilon)$. For a thin film, parameter

$\varepsilon = t/L$ is physically determined as the ratio of the film thickness t and its typical lateral dimension L (of the order of single domain size).

We study a three-dimensional thin film domain $V_\varepsilon = (\mathbf{x}', x_3)$, where $\mathbf{x}' = (x_1, x_2)$ belongs to the two-dimensional (2D) domain ω (the projection of the thin film on the plane) and $\varepsilon f(\mathbf{x}'/\varepsilon) < x_3 < \varepsilon[1 + f(\mathbf{x}'/\varepsilon)]$ with $\varepsilon > 0$ being a constant dimensionless film's thickness. We consider an arbitrary periodic modulation with the periodic cell given by a square of unit length. Typical examples of the surface shape functions that might be considered are $f(\mathbf{x}') = \sin^2(\pi x_1)$, $f(\mathbf{x}') = \sin^2(\pi x_1) \sin^2(\pi x_2)$, or the one shown in Fig. 1 (a).

In the continuum description the dimensionless micro-magnetic energy containing exchange and dipole-dipole interactions takes the form

$$\mathcal{E}_\varepsilon(\mathbf{M}) = \xi \int_{V_\varepsilon} |\nabla \mathbf{M}|^2 d\mathbf{x} + \int_{\mathbb{R}^3} |\nabla u|^2 d\mathbf{x}, \quad (2)$$

where $\xi = A/(\mu_0 M_s^2 L^2) > 0$ is the dimensionless material parameter, A is the exchange constant, μ_0 is vacuum permeability, M_s is saturation magnetization, and u in the dipolar contribution is determined as the unique solution satisfying

$$\Delta u = \text{div } \mathbf{M} \quad (3)$$

in the entire space, where the magnetization \mathbf{M} is nonzero only within the volume of the film.

To study the thin film limit, i.e. the limiting behavior of the energy as $\varepsilon \rightarrow 0$, it is convenient to consider the rescaled energy $E_\varepsilon(\mathbf{m}) = \mathcal{E}_\varepsilon(\mathbf{M})/\varepsilon$ with magnetization $\mathbf{M}(\mathbf{x}', x_3) = \mathbf{m}(\mathbf{x}', x_3/\varepsilon)$. In this limit, the main contribution to the energy is coming from the interaction of surface magnetic charges of the largest (top and bottom) surfaces. The limiting micromagnetic energy is given by the functional

$$E_0(\mathbf{m}) = \xi \int_\omega h^{\text{ex}}(\nabla \mathbf{m}) d\mathbf{x}' + \int_\omega K^{\text{eff}} \mathbf{m} \cdot \mathbf{m} d\mathbf{x}', \quad (4)$$

where a non-negative convex function h^{ex} vanishing at the origin is the exchange contribution [23], $K^{\text{eff}} = [K^{\text{hom}} + (K^{\text{hom}})^T]/2 = \{\kappa_{ij}\}$ is a symmetric 2nd-rank curvature induced effective anisotropy tensor with $i, j = 1, 2, 3$, and the homogenized anisotropy matrix K^{hom} takes the form

$$K^{\text{hom}} = \frac{1}{2\pi} \int d\mathbf{y}' \int_{\mathbb{R}^2} d\mathbf{z}' \mathbf{n}(\mathbf{y}') \otimes \mathbf{n}(\mathbf{z}' + \mathbf{y}') [g(0) - g(1)] \quad (5)$$

with

$$g(a) = \frac{1}{\sqrt{|\mathbf{z}'|^2 + |a + f(\mathbf{z}' + \mathbf{y}') - f(\mathbf{y}')|^2}} \quad (6)$$

and $\mathbf{n}(\mathbf{y}') = (-\nabla f(\mathbf{y}'), 1)$. Here the integration over \mathbf{y}' is performed in a unit square $[0, 1] \times [0, 1]$. We note that

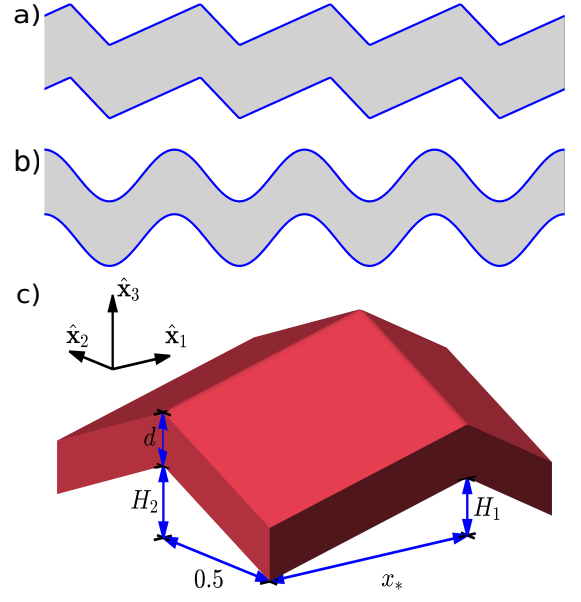


FIG. 2. (a) – (b) Cross-sections of thin films with periodic (a) pyramid and (b) $\sin^2 x_1 \sin^2 x_2$ textures. (c) One pyramid of the periodic structure shown in Fig. 1(a).

tensor K^{eff} is a non-negative definite, because the last term on the right-hand side of Eq. (4) is derived from the non-negative magnetostatic energy $\int_{\mathbb{R}^3} |\nabla u|^2$.

The main result of the Letter concerning the effective anisotropy behavior is based on Eqs. (5) and (6). In the following, we show that in thin magnetic films with periodic curvature one can engineer PMA or a uniaxial anisotropy of any particular orientation by choosing the surface shape $f(x_1, x_2)$ appropriately. This can open doors for tailoring the materials with a given anisotropy direction.

We first consider simpler, effectively one-dimensional (1D) case, when the 2D structure changes periodically only in one direction (we choose this direction to be $\hat{\mathbf{x}}_1$). In this case $f(x_1, x_2) = f(x_1)$ and after integrating Eq. (5) over y_2 and z_2 , we obtain

$$K_{1D}^{\text{hom}} = \frac{1}{4\pi} \int_0^1 dy_1 \int_{-\infty}^{\infty} dz_1 \mathbf{n}(y_1) \otimes \mathbf{n}(z_1 + y_1) \times \log \frac{z_1^2 + [1 + f(z_1 + y_1) - f(y_1)]^2}{z_1^2 + [f(z_1 + y_1) - f(y_1)]^2}. \quad (7)$$

It is easy to check in Eq. (7) that all effective matrix elements $\kappa_{i2} = \kappa_{2i} = 0$ and therefore zero is guaranteed to be the minimal eigenvalue of K^{eff} with the eigenvector $\hat{\mathbf{x}}_2$. If the zero eigenvalue is not degenerate, $\hat{\mathbf{x}}_2$ is the easy axis of anisotropy. Alternatively, if zero is an eigenvalue of multiplicity two, the anisotropy is of easy $x_1 x_2$ -plane type. For example, this is the case when $f(x_1) = \text{const}$. To conclude, for the structures periodically changing along x_1 direction, one can obtain only $x_1 x_2$ easy-plane or easy-axis anisotropy along $\hat{\mathbf{x}}_2$.

To explain the main ideas of how to engineer specific anisotropies, we next consider a truly 1D case by disregarding $\hat{\mathbf{x}}_2$ direction and investigating the anisotropy in the x_1x_3 -plane only. In this case K_{1D}^{eff} is reduced to 2×2 matrix

$$K_{1D}^{\text{eff}} = \begin{pmatrix} \kappa_{11} & \kappa_{13} \\ \kappa_{13} & \kappa_{33} \end{pmatrix}, \quad (8)$$

and the anisotropy orientation is determined by its eigenvalues and eigenvectors. If the minimal eigenvalue of K_{1D}^{eff} ,

$$\lambda_{\min} = (\kappa_{11} + \kappa_{33})/2 - \sqrt{(\kappa_{11} - \kappa_{33})^2/4 + \kappa_{13}^2}, \quad (9)$$

is not degenerate (i.e. $\kappa_{11} \neq \kappa_{33}$ or $\kappa_{13} \neq 0$), its eigenvector direction defines the easy axis of the anisotropy. Alternatively, if it is degenerate, the anisotropy is of x_1x_3 easy-plane type. For non-degenerate λ_{\min} , the anisotropy direction lies in x_1x_3 -plane and makes angle ϕ with $\hat{\mathbf{x}}_1$:

$$\phi = \arctan \left(\frac{1}{\gamma} \left[1 - \text{sgn}(\kappa_{33} - \kappa_{11}) \sqrt{\gamma^2 + 1} \right] \right) \quad (10)$$

for $\kappa_{11} \neq \kappa_{33}$, where $\gamma = 2\kappa_{13}/(\kappa_{33} - \kappa_{11})$, and in the special case $\kappa_{11} = \kappa_{33}$ and $\kappa_{13} \neq 0$ the angle $\phi = -\frac{\pi}{4} \text{sgn}(\kappa_{13})$.

To be more specific we consider 1D films whose profile is given on each period by a triangle, see Fig. 2 (a). Such a profile is completely characterized by the triangle's height H and the position of the top vertex x_* , so on $[0, 1]$ it is given by

$$f_1(x_1; H, x_*) = \begin{cases} H \frac{x_1}{x_*}, & 0 < x_1 \leq x_*, \\ H \frac{1-x_1}{1-x_*}, & x_* < x_1 \leq 1. \end{cases} \quad (11)$$

One can show analytically that by varying x_* and H it is possible to align the easy-axis anisotropy with any direction in x_1x_3 -plane. Here for simplicity we base our explanation on the results of numerical simulations presented in Fig. 3, where anisotropy angle ϕ as a function of triangle's height H is calculated for the periodic 1D structure given by Eq. (11). First, we notice that setting $H = 0$ results in the easy axis aligned with $\hat{\mathbf{x}}_1$. Figure 3 shows that increasing triangle's height H , while holding $x_* > 0.5$ fixed, continuously turns the easy axis from 0 to $\pi/2$. The special case of the symmetric triangles, $x_* = 0.5$, yields the easy-axis anisotropy along $\hat{\mathbf{x}}_1$ ($\phi = 0$) below the critical value of triangle's height $H_c \simeq 1.8$ and along $\hat{\mathbf{x}}_3$ ($\phi = \pi/2$) above H_c . For $H = H_c$ the anisotropy is of easy-plane type. Thus, the range $[0, \pi/2]$ for the anisotropy angles can be covered by varying x_* in a reasonable range above 0.5 and H from zero to large enough $H > H_c$. Now by changing parameter x_* from $x_* > 0.5$ presented in Fig. 3 to $x_* < 0.5$, due to the property $\phi(H, 1-x_*) = -\phi(H, x_*)$, we can rotate the easy axis anisotropy by $\pi/2$ and cover the range

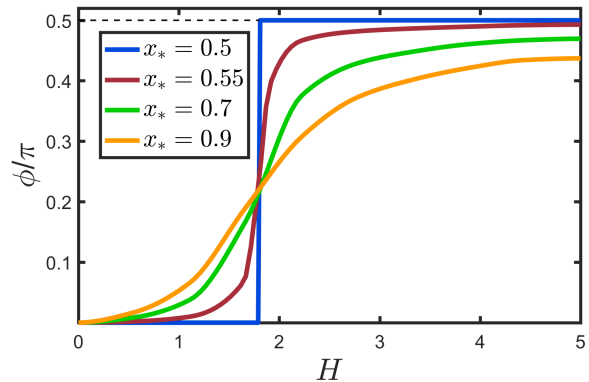


FIG. 3. Angle ϕ the anisotropy makes with $\hat{\mathbf{x}}_1$ as a function of triangle's height H in 1D case shown in Fig. 2 (a).

$[-\pi/2, 0]$. As a result we conclude that in 1D case one can cover the entire range $[-\pi/2, \pi/2]$ of the easy-axis anisotropy orientations in x_1x_3 -plane.

Next we study a more general case of 2D structures modulated in both $\hat{\mathbf{x}}_1$ and $\hat{\mathbf{x}}_2$ directions. Two examples of these periodic structures, made of pyramids and $\sin^2(x_1)\sin^2(x_2)$ functions, are shown in Fig. 1. To be more specific and show the essential physics, we concentrate on a periodic structure made of pyramids depicted in Fig. 2 (c). Such a pyramid on a base of a unit square $[0, 1] \times [0, 1]$ with the apex located at $(x_*, 0.5)$ is modeled by the function

$$f(x_1, x_2; H_1, x_*) = f_1(x_1; H_1, x_*) + f_2(x_2; H_2, 0.5), \quad (12)$$

where $f_{1,2}$ are given by Eq. (11). We choose in Eq. (12) the pyramid to be symmetric along x_2 , because it will be sufficient to show the essential features by varying the asymmetry only along x_1 . Since $f_2(x_2; H_2, 0.5)$ is a symmetric function, i.e. $f_2(x_2) = f_2(1-x_2)$, the anisotropy matrix takes the form

$$K^{\text{eff}} = \begin{pmatrix} \kappa_{11} & 0 & \kappa_{13} \\ 0 & \kappa_{22} & 0 \\ \kappa_{13} & 0 & \kappa_{33} \end{pmatrix}, \quad (13)$$

which is easy to show by exploiting the symmetries of Eq. (5). For Eq. (13), $\hat{\mathbf{x}}_2$ is always an eigenvector of K^{eff} with the eigenvalue κ_{22} . Hence, the other eigenvalues and eigenvectors of K^{eff} are determined by analyzing the reduced matrix given by Eq. (8) and have been already described in 1D case.

To confine the easy-axis to x_1x_3 -plane, it is sufficient to choose the parameters so that either of the conditions $\kappa_{11} < \kappa_{22}$ or $\kappa_{33} < \kappa_{22}$ is satisfied. For this we choose H_2 to be fixed and large enough, while H_1 and x_* are allowed to vary. Then, the anisotropy is of easy-axis type provided $\kappa_{11} \neq \kappa_{33}$ or $\kappa_{13} \neq 0$. Using similar arguments as in 1D case, we can show that it is possible to cover the

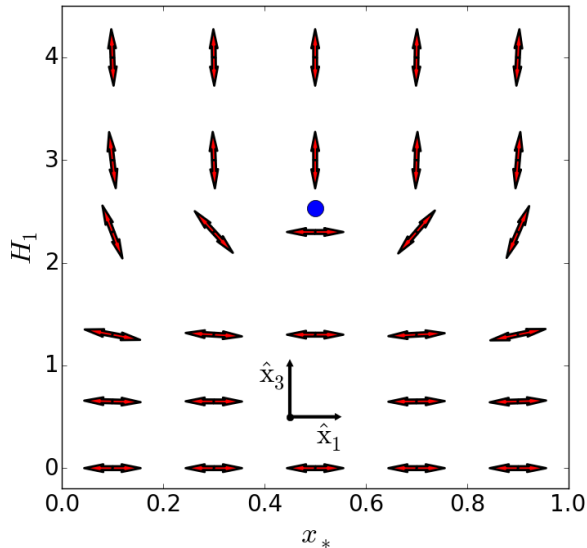


FIG. 4. Direction of anisotropy in the film depicted in Fig. 2 (c) as a function of pyramid's height H_1 and position of the apex x_* along \hat{x}_1 . The film lies in the x_1x_2 -plane and the base of each pyramid is a unit square.

entire range of directions in the x_1x_3 -plane. The corresponding results of numerical simulations using Monte-Carlo technique are presented in Fig. 4 which shows the picture qualitatively identical to the 1D problem. We numerically observe that the value $H_2 = 5$ is large enough in the above discussed sense and use it in the simulations. The value of H_c , where for $x_* = 0.5$ the anisotropy orientation abruptly changes from \hat{x}_1 to \hat{x}_3 , is found to be $\simeq 2.52$ for $H_2 = 5$; it is shown by the blue point in Fig. 4.

In order to obtain the preferred anisotropy in any direction it is enough to rotate pyramids by an appropriate angle in the x_1x_2 -plane and repeat the same arguments as above. Analogous results can be obtained for smooth 2D functions such as $\sin^2(\pi x_1) \sin^2(\pi x_2)$ shown in Fig. 1 (b), etc.

Discussion.- The result of this Letter shows that, in spite of conventional belief [24] that the dipole-dipole interaction in films thicker than a monolayer would put the magnetization in the plane of the film, in the case of particular surface modulation (or periodic roughness) this interaction can lead to perpendicular or any other uniaxial anisotropy. We note that the problem considered above with the same periodic profile on both surfaces can be extended even further. In the Supplementary material we provide the result derived for the more general case, where bottom and top profiles of the film are different [25]. Moreover, analogous homogenization technique may be used to treat two coupled magnetic films with periodically modulated surfaces [26, 27], this problem will be treated elsewhere [28].

A possible experimental confirmation of our findings is corroborated by recent observation of the giant enhancement of magnetic anisotropy in ultrathin (6 nm $\text{La}_{0.67}\text{Sr}_{0.33}\text{MnO}_3$ films grown on (001) SrTiO_3 substrates) manganite films via nanoscale 1D periodic depth modulation, where the top 2 nm were patterned into periodic stripes [29]. Generally, the magnetic systems studied in Ref. [30] may be excellent candidates for the curvature-induced anisotropy engineering.

The applicability limits of the asymptotic homogenization theory presented here are set by two scales: 1) the lower bound is determined by the validity of continuous model, i.e., it works on scales larger than interatomic spacing, 2) the upper bound is given by the scale of a single domain. Additionally, since the main complexity in determining the magnetic anisotropy is associated with understanding the influence of the magnetostatic energy, which is non-local, without loss of generality our method can be extended to additively include local terms such as Zeeman energy and crystalline anisotropy.

In summary, we have demonstrated that the perpendicular anisotropy can be achieved in thin ferromagnetic films solely due to an interplay of surface curvature and dipolar interactions. This points to the fact that the surface roughness may significantly modify anisotropy. We have shown how the nonlocal in their nature dipolar interactions, in the presence of arbitrary large surface curvature of the film, can be reduced to local effective anisotropy term in the magnetic energy. We modeled the film's surface shape by simple smooth functions $f(x_1, x_2)$, which can, in principle, be engineered in the films and demonstrated that by an appropriate choice of $f(x_1, x_2)$, one can orient the magnetic anisotropy axis along any direction. This provides a justification of a concept for future magnetic film nano-engineering with any chosen anisotropy without additional need of heavy-metal layers to provide spin-orbit coupling effects. This method would also allow to simplify the magnetic structures, by limiting them to only one magnetic layer.

O.A.T. acknowledges support by the Grants-in-Aid for Scientific Research (Grants No. 25800184, No. 25247056, and No. 15H01009) from the Ministry of Education, Culture, Sports, Science and Technology (MEXT) of Japan and SpinNet. V.S. and S.V. acknowledge support by the EPSRC Grant EP/K02390X/1.

* olegt@imr.tohoku.ac.jp

- [1] L. Néel, J. Phys. Radium **15**, 225 (1954).
- [2] A. J. Bennett and B. R. Cooper, Phys. Rev. B **3**, 1642 (1971).
- [3] H. Takeyama, K. P. Bohnen, and P. Fulde, Phys. Rev. B **14**, 2287 (1976).
- [4] M. Kolar, Phys. Status Solidi **96**, 683 (1979).
- [5] P. Bruno, J. Appl. Phys. **64**, 3153 (1988).

- [6] P. Bruno and J.-P. Renard, *Appl. Phys. A* **49**, 499 (1989).
- [7] G. H. O. Daalderop, P. J. Kelly, and M. F. H. Schuurmans, *Phys. Rev. B* **42**, 7270 (1990).
- [8] P. Bruno, *Phys. Rev. B* **39**, 865 (1989).
- [9] K. Kyuno, R. Yamamoto, and S. Asano, *J. Phys. Soc. Jap.* **61**, 2099 (1992).
- [10] D. S. Wang, R. Wu, and A. J. Freeman, *Phys. Rev. Lett.* **70**, 869 (1993).
- [11] D. S. Wang, R. Wu, and A. J. Freeman, *Phys. Rev. B* **48**, 15886 (1993).
- [12] S. Peng, M. Wang, H. Yang, L. Zeng, J. Nan, J. Zhou, Y. Zhang, A. Hallal, M. Chshiev, K. L. Wang, Q. Zhang, and W. Zhao, *Sci. Rep.* **5**, 18173 (2015).
- [13] D. Wu, Z. Zhang, L. Li, Z. Zhang, H. B. Zhao, J. Wang, B. Ma, and Q. Y. Jin, *Sci. Rep.* **5**, 12352 (2015).
- [14] Y. Gaididei, V. P. Kravchuk, and D. D. Sheka, *Phys. Rev. Lett.* **112**, 257203 (2014).
- [15] G. Carbou, *Math. Mod. Meth. Appl. Science* **11**, 1529 (2001).
- [16] V. Slastikov, *Math. Mod. Meth. Appl. Science* **15**, 1469 (2005).
- [17] A. Goussev, J. M. Robbins, V. Slastikov, and O. A. Tretiakov, *Phys. Rev. B* **93**, 054418 (2016).
- [18] R. Streubel, J. Lee, D. Makarov, M.-Y. Im, D. Kar-naushenko, L. Han, R. Schäfer, P. Fischer, S.-K. Kim, and O. G. Schmidt, *Advanced Materials* **26**, 316 (2014).
- [19] D. Makarov, M. Melzer, D. Kar-naushenko, and O. G. Schmidt, *Appl. Phys. Rev.* **3**, 011101 (2016).
- [20] A. Bedoya-Pinto, M. Donolato, M. Gobbi, L. E. Hueso, and P. Vavassori, *Appl. Phys. Lett.* **104**, 062412 (2014).
- [21] O. Lee, L. You, J. Jang, V. Subramanian, and S. Salahuddin, *Appl. Phys. Lett.* **107**, 252401 (2015).
- [22] R. Streubel, P. Fischer, F. Kronast, V. P. Kravchuk, D. D. Sheka, Y. Gaididei, O. G. Schmidt, and D. Makarov, *J. Phys. D: Appl. Phys.* **49**, 363001 (2016).
- [23] See the Supplementary Material for the exact analytical expression.
- [24] J. G. Gay and R. Richter, *Phys. Rev. Lett.* **56**, 2728 (1986).
- [25] See the Supplementary Material for the expression and more details.
- [26] L. Néel, *C. R. Acad. Sci., Paris* **255**, 1676 (1962).
- [27] B. D. Schrag, A. Anguelouch, S. Ingvarsson, G. Xiao, Y. Lu, P. L. Trouilloud, A. Gupta, R. A. Wanner, W. J. Gallagher, P. M. Rice, and S. S. P. Parkin, *Appl. Phys. Rev.* **77**, 2373 (2000).
- [28] M. Morini, V. Slastikov, and O. A. Tretiakov, unpublished.
- [29] A. Rajapitamahuni, L. Zhang, M. A. Koten, V. R. Singh, J. D. Burton, E. Y. Tsymbal, J. E. Shield, and X. Hong, *Phys. Rev. Lett.* **116**, 187201 (2016).
- [30] D. K. Ball, K. Lenz, M. Fritzsche, G. Varvaro, S. Günther, P. Krone, D. Makarov, A. Mücklich, S. Facko, J. Fassbender, and M. Albrecht, *Nanotech.* **25**, 085703 (2014).